OVERVIEW OF RESULTS FROM NA61/SHINE: UNCOVERING CRITICAL STRUCTURES*

Marek Gazdzicki[a,b], Andrzej Rybicki[c]

for the NA61/SHINE Collaboration

[a]Goethe University, Frankfurt, Germany
[b]Jan Kochanowski University, Kielce, Poland
[c]Institute of Nuclear Physics Polish Academy of Sciences
31-342 Kraków, Poland

(Received May 30, 2019)

NA61/SHINE is a multi-purpose experiment to study hadron–proton, hadron–nucleus and nucleus–nucleus collisions at the CERN Super Proton Synchrotron. The experiment performs unique measurements for physics of strong interactions as well as important reference measurements for neutrino and cosmic-ray physics. The results from the strong interaction programme uncover rapid changes in collision-energy and system-size dependence of basic hadron production properties — the *critical structures*. They are attributed to the onset of deconfinement, onset of fireball and may indicate the critical point of strongly interacting matter.

DOI:10.5506/APhysPolB.50.1057

1. Introduction

NA61/SHINE (the "SPS Heavy Ion and Neutrino Experiment") is a fixed target particle and high-energy nuclear physics experiment at the CERN Super Proton Synchrotron (SPS) [1]. The experiment studies identified hadrons produced in hadron–hadron, hadron–nucleus, and nucleus–nucleus collisions. A large variety of beam particles and nuclei, a hydrogen target, and a variety of nuclear targets are available [2].

NA61/SHINE is a large acceptance spectrometer with good charge hadron identification, and almost complete coverage in the projectile hemisphere in the collision c.m.s. A visualization of the main parts of the detector setup is presented in Fig. 1 (a). The main component of NA61/SHINE is a system of eight Time Projection Chambers (TPCs), some of which are being placed in a strong (up to 1.5 T) magnetic field which ensures precise measurement of the momentum vector of charged particles. In a limited phase

* Presented at the Cracow Epiphany Conference on Advances in Heavy Ion Physics, Kraków, Poland, January 8–11 2019.

space, charged particle identification is supplemented by the Time-of-Flight walls. Nucleus–nucleus collisions are classified by the energy deposit of projectile remnants (spectators) measured in the forward calorimeter (Proton Spectator Detector, PSD). The most central collisions deposit the smallest energy.

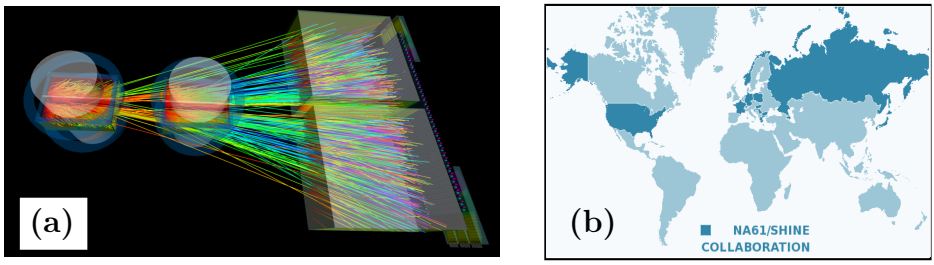

Fig. 1. (a) Virtual reality visualization of a single Xe+La collision at 150 A GeV/c beam momentum, and the main elements of the NA61/SHINE detector setup. (b) The NA61/SHINE Collaboration. Both plots are taken from Ref. [2].

The physics goals of the NA61/SHINE Collaboration (Fig. 1 (b)) are realized in the framework of the three research programmes.

The *neutrino programme* consists in measurements of proton–nucleus and pion–nucleus interactions, made in order to determine parameters of neutrino beams produced from impinging protons at J-PARC, Japan, and Fermilab, USA. NA61/SHINE significantly reduces the systematic uncertainties of neutrino flux, which constitute a key issue in studies of neutrino properties in accelerator neutrino experiments. A review of this programme can be found in Ref. [3]. Its extensions for the period of 2021–2024 are improved measurements of particle production with the replica of DUNE and T2K targets, and studies of production of hadrons at low momentum beams [4].

The *cosmic ray programme* consists of measurements of particle production in hadron–carbon interactions, which serves as an approximation of what happens when hadrons interact with air nuclei. This information improves the understanding of nuclear cascades in air showers, needed in studies of extragalactic, very high energy protons and nuclei made by the Pierre Auger Observatory and KASKADE experiments. A summary of the present achievements of this programme can be found in Ref. [5]. A recent extension here are reference measurements of nuclear fragmentation cross sections for cosmic ray experiments located in space. The uncertainties of the latter constitute a significant limitation for the understanding of comic ray propagation. NA61/SHINE is expected to significantly reduce these uncertainties (from 20% down to about 0.5%). This activity, planned after the year 2020 and presently recommended by the SPS Committee, is described in Ref. [4].

The present paper presents a limited selection of results from the third, *strong interactions* programme. It consists in detailed studies of effects induced by strong and electromagnetic forces in nucleus–nucleus, proton–proton and proton–nucleus collisions. The programme's original aim was to investigate properties of the transition between the quark–gluon plasma and hadron gas by collision energy scans with various beam and target nuclei, as well as the search for the critical point (CP) of strongly interacting matter. As it will be shown below, a specific pattern of transitions of the latter strongly interacting matter (the *critical structures*) appears to emerge from these studies.

We note that the present review is partially based on Ref. [6], and can be considered as an extension and update of the results presented therein.

2. The critical structures

The non-perturbative nature of strong interactions makes the investigation of the phase diagram of QCD one of the most challenging tasks in physics. The NA61/SHINE Collaboration fulfills this task by a two-dimensional scan of the (μ, T) phase diagram, Fig. 2 (left), by varying the beam momentum and the colliding system size. The total dataset collected by the strong interaction programme is displayed in Fig. 2 (right). As it is apparent from the figure, it constitutes an important reference point for the less versatile but high statistics datasets collected at the LHC energies, as well as for RHIC energies where an almost comparably versatile dataset has been collected, see Ref. [7].

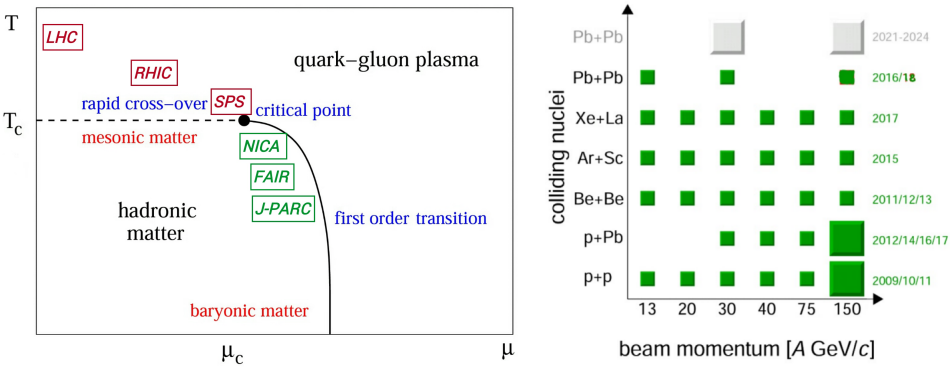

Fig. 2. (Colour on-line) Left: the phase diagram of strongly interacting matter drawn as a function of baryochemical potential μ and temperature T [8]. Right: total set of reactions collected (grey/green) and planned for measurement (light grey) by the NA61/SHINE Collaboration [2].

2.1. The onset of deconfinement

The discovery of the onset of deconfinement (the localization of the nucleus–nucleus collision energy above which the formation of the quark–gluon plasma becomes possible) was achieved by the NA49 Collaboration [9]. The study consisted in measuring the characteristic structures in the energy dependence of specific observables predicted by the Statistical Model of the Early Stage (SMES [10]), in central Pb+Pb collisions. The recent results from NA61/SHINE on the system size dependence of these structures bring new information which may have profound consequences for the understanding of the nature of the onset of deconfinement.

The energy dependence of the K^+/π^+ ratio measured at mid-rapidity in Pb+Pb, Au+Au, Be+Be and p+p collisions is presented in Fig. 3 (a). The onset of deconfinement is apparent in the characteristic, non-monotonic behaviour of the strangeness over pion ratio in central heavy-ion collisions. However, new data from NA61/SHINE suggest a somewhat similar, bend-like structure also for the relatively very small system produced in proton–proton reactions. The positions of the heavy-ion "horn" and the p+p "bend" coincide in terms of the collision energy $\sqrt{s_{NN}}$.

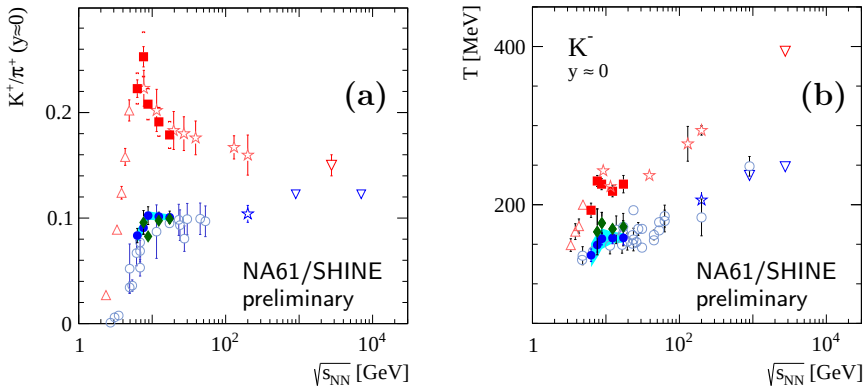

Fig. 3. (Colour on-line) (a) Compilation of experimental data on the K^+/π^+ ratio and (b) inverse slope parameter T for K^- in Pb+Pb and Au+Au (grey/red), Be+Be (green diamonds) and p+p (black/blue) reactions. Closed symbols mark NA49 and NA61/SHINE data. Open symbols indicate all other "world" data (see Ref. [11] for a detailed reference list).

Complementary to the above, Fig. 3 (b) displays the energy dependence of the inverse slope T, obtained from the fit to the produced negative kaon m_{T} distribution. In central heavy-ion collisions, this "apparent temperature" displays a characteristic step-like behaviour which can be considered as a strong interaction analogy of the ice-water phase transition. Surprisingly, the same statement seems valid for the proton–proton system.

Here, it should be pointed out that, since 2017, it is known that high multiplicity p+p events at the LHC energies display specific properties which were up to now attributed to deconfined quark matter created in heavy-ion collisions [12]. It seems, therefore, justified to ask the question whether the characteristic structures apparent in Fig. 3 are to be attributed, in p+p collisions, to a phenomenon similar to the onset of deconfinement in heavy-ion reactions. Further studies, including high statistics measurements of p+p collisions in the SPS energy range, can help to clarify this matter.

As a consequence of the above, the energy dependence of proton–proton and nucleus–nucleus collisions suggests the characteristics of the *first* critical structure in strongly interacting matter at SPS energies — the onset of deconfinement — is well-established for collisions involving heavier nuclei. Its presence and interpretation are for the time being still open in small systems like p+p reactions. The *second* critical structure will be discussed in the subsequent section.

2.2. The onset of fireball

This second structure is attributed to the *beginning of creation of large clusters of strongly interacting matter* in nucleus–nucleus (A+A) collisions with increasing nuclear mass number (A). A schematic explanation is shown in Fig. 4. Starting from p+p collisions ($A = 1$), particle production will originate from small clusters; the average cluster volume will remain constant as a function of A until a limiting value at which these will start to merge into a single large cluster of strongly interacting matter (SIM), the fireball. This *onset of fireball* [13] should evidently reflect in observables sensitive to the mean cluster volume $\langle V_C \rangle$. Following statistical model predictions (see *e.g.* Ref. [14]), such a quantity is the kaon over pion ratio.

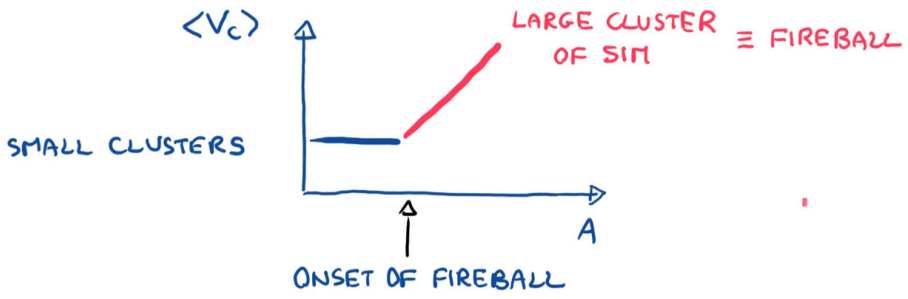

Fig. 4. Schematic drawing of the onset of fireball as a function of the mass number A of the colliding nuclei in A+A collisions. $\langle V_C \rangle$ stands for the mean volume of clusters created in the collisions.

The positive kaon over pion ratio at beam momentum of 30 A GeV/c ($\sqrt{s_{NN}}$ = 7.7 GeV) is shown in Fig. 5. The system size dependence of the experimental data is clearly reminiscent of the scheme shown in Fig. 4.

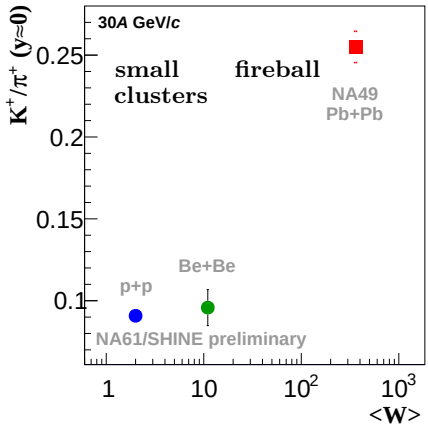

Fig. 5. Mid-rapidity K^+/π^+ ratio as a function of the mean number $\langle W \rangle$ of wounded nucleons in the system created by minimum bias p+p, central Be+Be and central Pb+Pb collisions at 30 A GeV/c beam momentum [11].

The theoretical calculations obtained within the framework of UrQMD and Canonical Ensemble Hadron Resonance Gas (CE HRG) models [16] are shown in Fig. 6. Both these state-of-the-art models clearly fail to reproduce the data. What is noteworthy in Fig. 6 (a) is the apparent success of the Wounded Nucleon Model [15] in the description of the K^+/π^+ ratio from p+p up to central Be+Be reactions, which suggests the latter range as the extent of the *small clusters* regime from Fig. 4. This is confirmed in Fig. 7 which shows the system size dependence of the positive kaon over pion ratio at the top SPS beam momentum (150–158 A GeV/c, which corresponds to $\sqrt{s_{NN}}$ = 16.8–17.2 GeV). Here, although with large error bars, the experimental data on C+C, Si+Si and Pb+Pb collisions suggest the rise of the K/π ratio as a function of the increasing size of the system, corresponding to the *fireball* regime of particle production pointed in Fig. 4.

Account taken that no C+C nor Si+Si experimental data are available at the lower collision energy shown in Fig. 5, the similarity of the system size dependence of the strangeness over pion ratio from p+p through Be+Be up to Pb+Pb collisions is noteworthy in Figs. 5 and 7 (a). Within the present (sizeable) uncertainties, this suggests the onset of fireball to be located at the same system size of about $\langle W \rangle$ = 10–20 wounded nucleons at both collision energies.

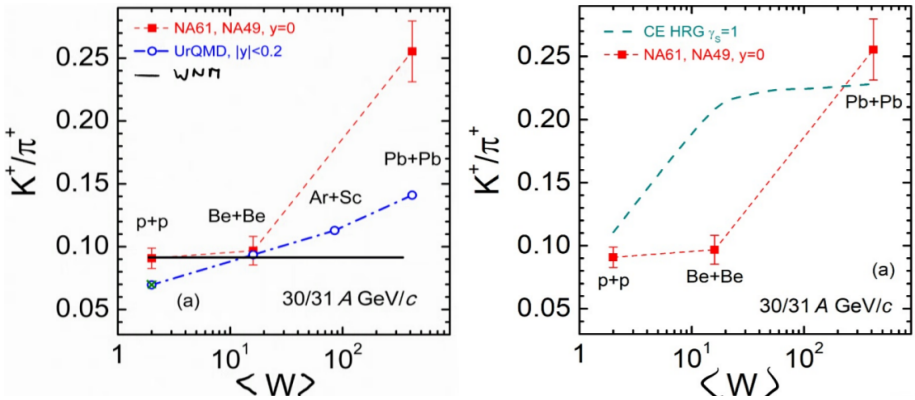

Fig. 6. Experimental data from Fig. 5 compared to calculations obtained in the framework of UrQMD and CE HRG models. The horizontal line in panel (a) indicates the prediction of the Wounded Nucleon Model [15]. The figure is redrawn from Ref. [16].

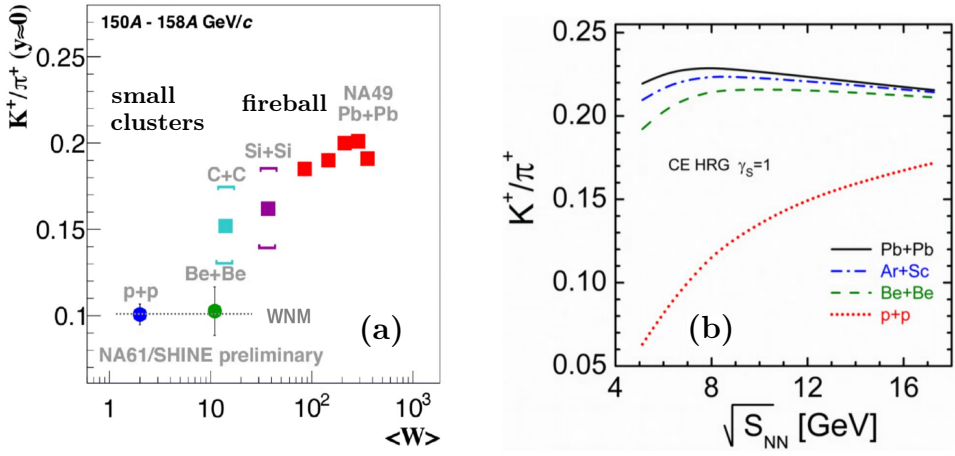

Fig. 7. (a) Mid-rapidity K^+/π^+ ratio as a function of the mean number $\langle W \rangle$ of wounded nucleons in the colliding system created by minimum bias p+p collisions and various A+A reactions at 150 A–158 A GeV/c beam momentum [6]. (b) Predictions of the CE HRG model (see the text) for the energy dependence of the K^+/π^+ ratio in p+p and various A+A collisions [16].

For completeness, we note that the above similarity as a function of collision energy is again in contradiction with the CE HRG model shown in Fig. 7 (b). The latter model predicts a large increase in the K/π ratio between p+p and Be+Be collisions in disagreement with the NA61/SHINE data, and fails to reproduce the $\sqrt{s_{NN}}$-dependence shown in Fig. 7 (a).

Summarizing Secs. 2.1 and 2.2, we tentatively conclude on the position of the *two critical structures* on the system size *versus* collision energy plane as it is drawn in Fig. 8. The position of the onset of fireball seems to be energy-independent in the SPS range. The onset of deconfinement from hadronic matter to quark–gluon plasma is well-established in the *fireball* region at high mass A of the colliding nuclei, while its presence in the *small clusters* regime is for the time being still open and remains to be elucidated.

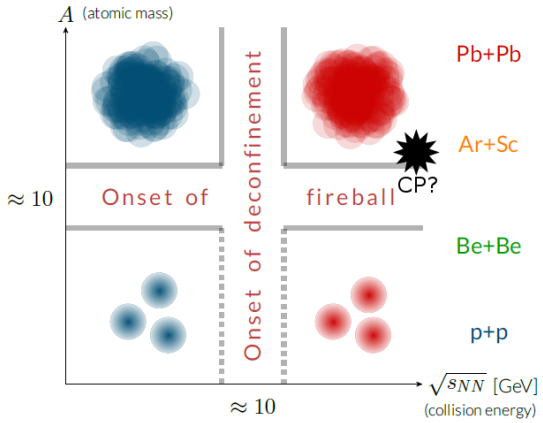

Fig. 8. Onset of deconfinement and onset of fireball as a function of collision energy and system size [14]. The position of the critical point which could be implied by the NA49 and NA61/SHINE intermittency studies (see the text) is also indicated in the plot.

2.3. The critical point of strongly interacting matter

In the phase diagram of strongly interacting matter shown in Fig. 2 (a), the critical point (CP) marks the change of properties in the transition between hadronic matter and quark–gluon plasma, from the first order transition to cross-over with decreasing baryochemical potential. The experimental localization of the critical point is supposed to consist in the measurement of the "hill of fluctuations" as a function of colliding system size and energy, as illustrated in Fig. 9. This is subject to three main conceptual difficulties:

1. The high-energy nucleus–nucleus collision can be considered as a trajectory on the phase diagram, bringing the system into the QGP and back to the hadronic phase. Therefore, the localization of the critical point must consist in measuring a reaction which, at the moment of the transition from the QGP to the hadronic phase (that is, at freeze-out), is placed in the configuration (μ, T) corresponding to the CP. This constitutes a serious challenge, account taken of the practical

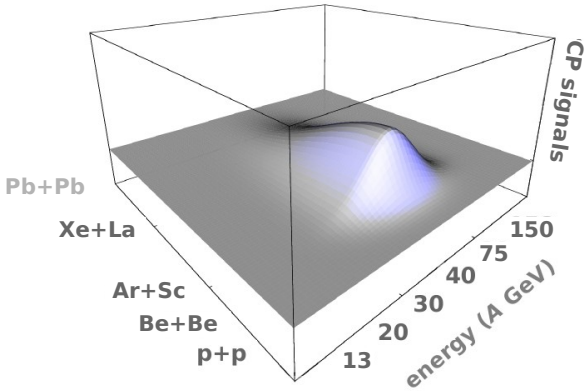

Fig. 9. Theoretical studies predict the presence of a "hill of fluctuations" as a function of colliding system size and energy, for observables sensitive to the critical point (see Ref. [8] for more details).

limitations in the number of possible nucleus–nucleus systems measured in the system size *versus* collision energy plane (Fig. 2 (b)). The latter statement is particularly valid in view of theoretical arguments suggesting the narrowness of the critical region [17].

2. The presence of the two other critical structures in the system size *versus* collision energy plane creates a phenomenological ambiguity evident from Fig. 8. In the case the CP is located in close vicinity of the onset of fireball or onset of deconfinement, its identification and differentiation from a possible reflection of one of these two structures may constitute a significant challenge for theory [18].

3. Finally, the experimental measurement of potentially critical fluctuations must be accompanied by a theoretical exclusion of possible non-critical effects induced by the strong interaction, like these relevant to HBT phenomena [19].

The principal result from NA61/SHINE in its search for the critical point is the indication for fluctuations of proton density, resulting in intermittent behaviour [22–25] of factorial moments $F_2(M)$ in semi-central Ar+Sc collisions at the top SPS energy. This is shown in Fig. 10. This confirms a similar observation in Si+Si collisions located in a nearby position on the phase diagram from the NA49 experiment [21]. No conclusive signal was found up to now in Be+Be, C+C, and Pb+Pb reactions as discussed in these proceedings [26]. A detailed account of the experimental analysis can be found therein.

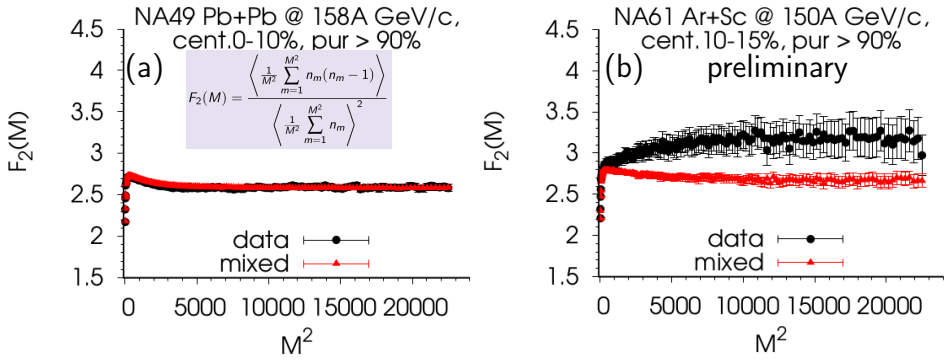

Fig. 10. (Colour on-line) Factorial moments $F_2(M)$ for protons produced close to mid-rapidity in (a) Pb+Pb and (b) Ar+Sc reactions, for experimental data (black) and mixed events (grey/red). The factorial moments are drawn as a function of the number M^2 of (p_x, p_y) cells, where p_x and p_y are the transverse components of the proton momentum vector. From Refs. [20, 21].

If it is confirmed by future studies, this preliminary result from the NA61/SHINE experiment can point at the localization of the critical point close to the (μ, T) configuration of Ar+Sc reactions at the top SPS energy, as indicated in Fig. 8. However, this is to be taken with caution in view of the inherent complexity of the experimental analysis [26], as well as of the necessity of exclusion of possible non-critical sources for the behaviour shown in Fig. 10 (a). Active experimental work, aimed at the further clarification of the energy and system size dependence of proton factorial moments $F_2(M)$, and at the assessment of the significance of this result, is presently in progress in NA61/SHINE.

Sections 2.1–2.3 outlined the main results of the strong interaction programme in terms of bulk phenomena occurring in the central kinematic region of the reaction. Complementary studies, aimed at investigating the longitudinal evolution of the system by measuring electromagnetic (EM) effects, particle spectra and collective flow phenomena, are also described in these proceedings [27]. Measurements planned in the nearest future will be addressed below.

3. Plans for the period 2020–2024

The planned measurements include:

(1) open charm measurements in Pb+Pb collisions;

(2) precise measurements of electromagnetic effects.

This section will focus only on item (1). For item (2), the reader is asked to refer to another paper in these proceedings [27], as well as to Ref. [4].

The aim of the open charm measurements (see Ref. [4] for a more precise description) is to obtain the first data on the mean number of $c\bar{c}$ pairs produced in the full phase space available to the heavy-ion reaction. The programme also aims at providing the first data on the energy and system size of charmed quark (mostly D meson) production. The fundamental need for these new measurements originates from the following premises:

1. *The mechanism of open charm production* is, at present, known with uncertainties reaching about two orders of magnitude as illustrated in Fig. 11 (a) which gives a compilation of results obtained by different available models in Pb+Pb collisions at the top SPS energy. It is evident that precise experimental data will constitute a qualitative breakthrough in terms of narrowing the spectrum of acceptable models and, therefore, understanding the mechanisms of c and $\bar{c}$ production.

2. *Deconfined matter* is expected to differ from confined matter in terms of c and $\bar{c}$ production. This originates from the different masses of the lightest charge carriers which are D mesons in the confined and c quarks in the deconfined phase. An example is given in Fig. 11 (b), which illustrates the corresponding predictions from the Statistical Model of the Early Stage (see Sec. 2.1 for comparison).

3. *The suppression of J/Ψ production in Pb+Pb collisions*, an important argument for the discovery of a new state of matter announced by CERN in the year 2000 [28], was claimed on the basis of the assumption of the proportionality of mean $c\bar{c}$ pair multiplicity to that of average multiplicity of Drell–Yan pairs: $\langle c\bar{c} \rangle \sim \langle \mathrm{DY} \rangle$. This may be incorrect due to effects such as shadowing or parton energy loss [29]. The clarification of this important issue requires new experimental data on c and $\bar{c}$ rather than Drell–Yan production. Figure 11 (c) presents the original data on J/Ψ suppression [38], put together with the estimate of accuracy of the new result obtained using the future open charm measurement from NA61/SHINE.

The planned measurement of open charm production requires a very significant upgrade of the NA61/SHINE detector which is presently in progress. Details on the upgrade programme can be found in Ref. [4]. A prototype vertex detector, Fig. 12 (a), is already in operation. The (K, π) invariant mass spectrum reconstructed from test data taken with this prototype detector gives a clear indication of a $(D^0 + \bar{D}^0)$ peak as shown in Fig. 12 (b), demonstrating the feasibility of the open charm measurement by the NA61/SHINE Collaboration.

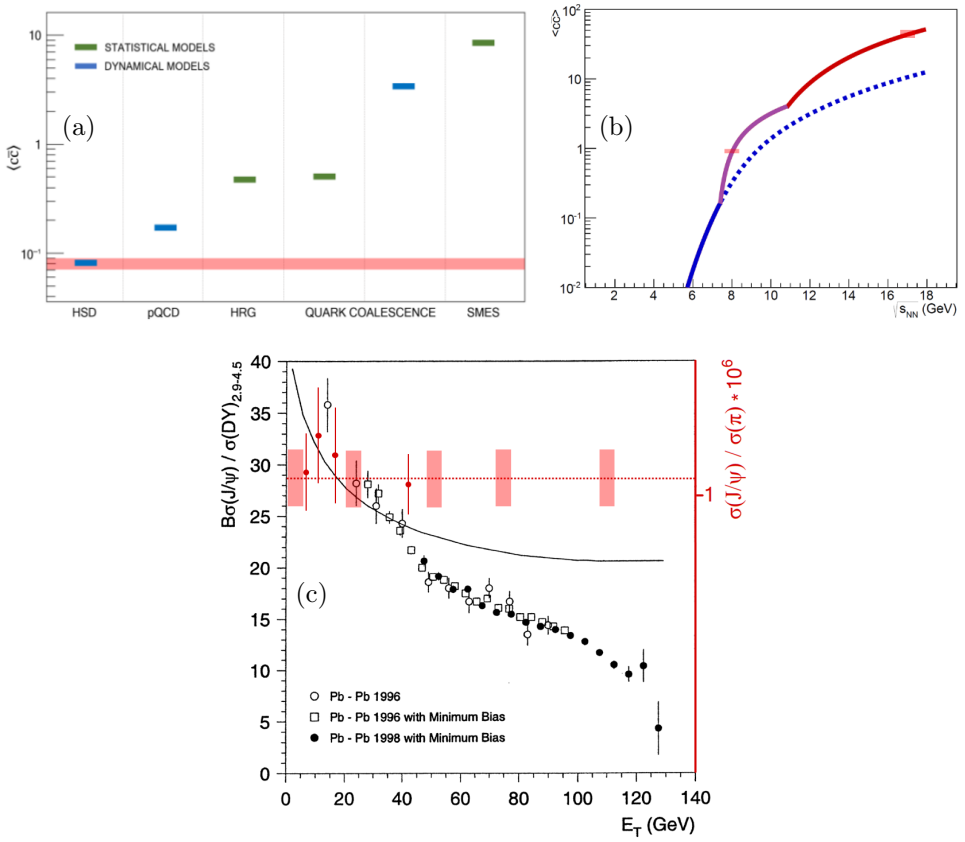

Fig. 11. (Colour on-line) (a) Mean multiplicity of charm quark pairs, produced in full phase space in central Pb+Pb collisions at 158 A GeV/c beam momentum, obtained from dynamical models (grey/blue bars): HSD [30, 31], pQCD-inspired [32, 33], and Dynamical Quark Coalescence [34], compared with results from statistical models (light grey/green bars): Hadron Resonance Gas [35], Statistical Quark Coalescence [35], and SMES [10]. (b) Energy dependence of $\langle c\bar{c} \rangle$ in central Pb+Pb collisions, calculated within the SMES model [36, 37]. The black/blue line corresponds to confined, the grey/purple line to mixed phase, and the light grey/red line to deconfined matter. The dashed line presents the prediction with no phase transition. (c) The ratio of $\sigma(J/\Psi)/\sigma(\mathrm{DY})$ as a function of transverse energy (a measure of centrality, or collision violence) in Pb+Pb collisions at 158 A GeV measured by NA50. The curve represents the J/Ψ suppression due to ordinary nuclear absorption [38]. Grey/red bars mark the expected accuracy of the $\sigma(J/\Psi)/\sigma(c\bar{c})$ result of NA61/SHINE. All the panels are redrawn from Ref. [4].

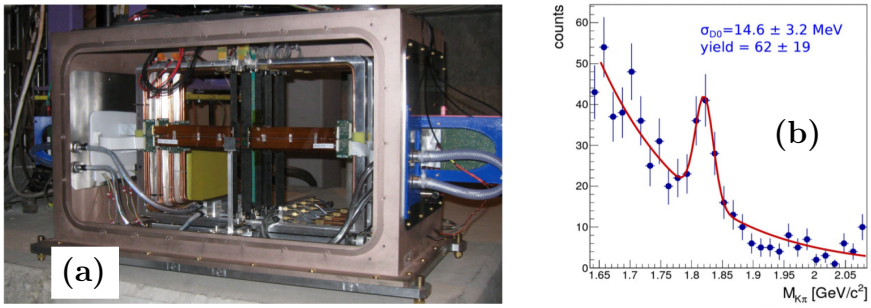

Fig. 12. (a) Prototype Small Acceptance Vertex Detector for NA61/SHINE [4]. (b) The invariant mass spectrum of D^0 and $\bar{D}^0$ candidates obtained in a test run on central Pb+Pb collisions at 150 A GeV/c beam momentum [39].

4. Summary

The unique position of the NA61/SHINE experiment in the heavy-ion field is given by the detector capabilities, combined with its position on the phase diagram of strongly interacting matter defined by the available system sizes and collision energies. The analysis of NA61/SHINE data available up to now suggests the presence of different critical structures as a function of system volume and energy. The system size dependence, not described by the models tested up to now, is attributed to the transition from a superposition of small clusters into a large cluster of strongly interacting matter — the onset of fireball. The onset of deconfinement, that is, the threshold for quark–gluon plasma production is well-defined for large system sizes (in the fireball regime). Its presence is still open and remains to be clarified for small systems (in the small cluster regime). New data on intermittent behaviour of proton density in Ar+Sc reactions can constitute a first indication for the critical point from NA61/SHINE, but final data on this observable must be accompanied by the theoretical exclusion of possible non-critical phenomena at the origin of the observed effect.

In the near future, NA61/SHINE is the only experiment able to measure open charm production in heavy-ion collisions in full available phase space.

This work was supported by the National Science Centre, Poland (NCN) (grants Nos. 2014/14/E/ST2/00018, 2015/18/M/ST2/00125, and 2018/30/A/ST2/00226).

REFERENCES

[1] A. Aduszkiewicz *et al.* [NA49-future Collab.], CERN-SPSC-2006-034.
[2] Home page of the NA61/SHINE Collab., http://shine.web.cern.ch/

[3] Y. Nagai, arXiv:1810.01366 [physics.ins-det].
[4] A. Aduszkiewicz *et al.* [NA61/SHINE Collab.], CERN-SPSC-2018-008.
[5] M. Unger [NA61/SHINE Collab.], *Nucl. Part. Phys. Proc.* **279**, 118 (2016).
[6] A. Rybicki [NA61/SHINE Collab.], *Acta Phys. Pol. B Proc. Suppl.* **12**, 425 (2019).
[7] R. Belmont [PHENIX Collab.], *Acta Phys. Pol. B* **50**, 1003 (2019), this issue.
[8] M. Gazdzicki, P. Seyboth, *Acta Phys. Pol. B* **47**, 1201 (2016) and references therein.
[9] S.V. Afanasiev *et al.* [NA49 Collab.], *Phys. Rev. C* **66**, 054902 (2002).
[10] M. Gazdzicki, M.I. Gorenstein, *Acta Phys. Pol. B* **30**, 2705 (1999).
[11] K. Grebieszkow [NA61/SHINE Collab.], arXiv:1904.03165 [nucl-ex].
[12] J. Adam *et al.* [ALICE Collab.], *Nature Phys.* **13**, 535 (2017).
[13] The name was proposed by Edward Shuryak at CPOD 2017 in Stony Brook.
[14] M. Gazdzicki [NA61/SHINE Collab.], *PoS* **CPOD2017**, 012 (2018).
[15] A. Białas, M. Bleszyński, W. Czyż, *Nucl. Phys. B* **111**, 461 (1976).
[16] A. Motornenko *et al.*, *Phys. Rev. C* **99**, 034909 (2019) and references therein.
[17] N.G. Antoniou, F.K. Diakonos, *J. Phys. G* **46**, 035101 (2019).
[18] L. Turko, private communication.
[19] A. Bzdak, private communication.
[20] N. Davis [NA61/SHINE Collab.], *PoS* **CPOD2017**, 030 (2018).
[21] T. Anticic *et al.* [NA49 Collab.], *Eur. Phys. J. C* **75**, 587 (2015).
[22] A. Białas, R. Peschanski, *Nucl. Phys. B* **273**, 703 (1986).
[23] J. Wosiek, *Acta Phys. Pol. B* **19**, 863 (1988).
[24] A. Białas, R.C. Hwa, *Phys. Lett. B* **253**, 436 (1991).
[25] N.G. Antoniou *et al.*, *Phys. Rev. Lett.* **97**, 032002 (2006).
[26] N. Davis, *Acta Phys. Pol. B* **50**, 1029 (2019), this issue.
[27] A. Marcinek, *Acta Phys. Pol. B* **50**, 1127 (2019), this issue.
[28] U.W. Heinz, M. Jacob, arXiv:nucl-th/0002042.
[29] H. Satz, *EPJ Web Conf.* **71**, 00118 (2014).
[30] O. Linnyk *et al.*, *Int. J. Mod. Phys. E* **17**, 1367 (2008).
[31] T. Song, private communication.
[32] R.V. Gavai *et al.*, *Int. J. Mod. Phys. A* **10**, 2999 (1995).
[33] P. Braun-Munzinger, J. Stachel, *Phys. Lett. B* **490**, 196 (2000).
[34] P. Levai *et al.*, *J. Phys. G* **27**, 703 (2001).
[35] A.P. Kostyuk *et al.*, *Phys. Lett. B* **531**, 195 (2002).
[36] R.V. Poberezhnyuk *et al.*, *Acta Phys. Pol. B* **48**, 1461 (2017).
[37] R.V. Poberezhnyuk, private communication.
[38] M.C. Abreu *et al.* [NA50 Collab.], *Phys. Lett. B* **477**, 28 (2000).
[39] P. Staszel [NA61/SHINE Collab.], *Nucl. Phys. A* **982**, 879 (2019).